The Canadian Journal of Mineralogy and Petrology
ISSN 2817-1713
Vol. 61, pp. 177-188 (2023)
DOI: 10.3749/2200039

BETZITE, $Na_6Ca_2(Al_6Si_6O_{24})Cl_4$, A NEW CANCRINITE-GROUP MINERAL FROM THE EIFEL PALEOVOLCANIC REGION, GERMANY

NIKITA V. CHUKANOV[§]

Federal Research Center of Problems of Chemical Physics and Medicinal Chemistry, Russian Academy of Sciences, Semenova Str. 1, Chernogolovka, Moscow Region, 142432 Russia
Faculty of Geology, Moscow State University, Vorobievy Gory, 119991 Moscow, Russia

NATALIA V. ZUBKOVA

Faculty of Geology, Moscow State University, Vorobievy Gory, 119991 Moscow, Russia

OLGA N. KAZHEVA

Laboratory of Arctic Mineralogy and Material Sciences, Kola Science Centre, Russian Academy of Sciences, 14 Fersman str., Apatity 184209 Russia

DMITRY A. VARLAMOV

Institute of Experimental Mineralogy RAS, Chernogolovka, 142432 Russia

IGOR V. PEKOV

Faculty of Geology, Moscow State University, Vorobievy Gory, Moscow, 119991, Russia

DMITRIY I. BELAKOVSKIY

Fersman Mineralogical Museum of Russian Academy of Sciences, Leninskiy Prospekt 18-2, Moscow, 119071 Russia

BERND TERNES

Bahnhofstrasse 45, 56727 Mayen, Germany

WILLI SCHÜLLER

Im Straussenpesch 22, 53518 Adenau, Germany

SERGEY N. BRITVIN

Department of Crystallography, St Petersburg State University, University Embankment 7/9, 199034 St Petersburg, Russia

DMITRY YU. PUSHCHAROVSKY

Faculty of Geology, Moscow State University, Vorobievy Gory, 119991 Moscow, Russia

ABSTRACT

Betzite, ideally $Na_6Ca_2(Al_6Si_6O_{24})Cl_4$, a new cancrinite-group mineral, was discovered in a metasomatically altered (pyrometamorphosed) calcic xenolith, hosted by alkaline basalt at the Bellerberg paleovolcano in the Eastern Eifel region, Rhineland-Palatinate, Germany. The associated minerals are anorthite, phlogopite, diopside, grossular, fluorite, calcite, a

[§] *Corresponding author e-mail address*: chukanov@icp.ac.ru

tobermorite-like mineral, and vanadoallanite-(Ce). Betzite occurs as colorless hexagonal prismatic crystals up to 2 mm long and up to 0.5 mm thick. The new mineral is brittle, with a Mohs' hardness of 5½. Distinct cleavage on $\{10\bar{1}0\}$ and parting on $\{0001\}$ are observed. The $D_{meas} = 2.38(2)$ g/cm^3 and $D_{calc} = 2.363$ g/cm^3. Betzite is optically uniaxial (+) with $\omega = 1.528(2)$ and $\varepsilon = 1.545(3)$. The IR spectrum is given. The chemical composition of betzite is (wt.%; electron microprobe, H_2O determined by the modified Penfield method): Na_2O 11.88, K_2O 4.82, CaO 10.74, MgO 0.21, Al_2O_3 27.32, Fe_2O_3 0.68, SiO_2 32.84, SO_3 1.89, Cl 10.48, H_2O 1.10, $-O\equiv Cl$ –2.37, total 99.59. The empirical formula is $Na_{4.22}K_{1.13}Ca_{2.11}Mg_{0.06}(Si_{6.01}Al_{5.90}Fe^{3+}_{0.09}O_{24})Cl_{3.25}(SO_4)_{0.26}(H_{1.34}O_{0.64})$. The crystal structure was determined using single-crystal X-ray diffraction data. It is hexagonal, space group $P6_3$, $a = 12.8166(9)$ Å, $c = 5.3562(3)$ Å, $V = 761.95(12)$ Å^3 (at a temperature of 100 K) and $Z = 3$. Betzite is a dimorph of quadridavyne, with a disordered distribution of extra-framework components occupying channels. The strongest lines of the powder X-ray diffraction pattern [*d,* Å (*I*, %) (*hkl*)] are: 11.14 (31) (100), 4.833 (93) (101), 3.715 (95) (300), 3.313 (100) (211), 2.787 (37) (400), 2.681 (56) (002, 131), 2.474 (35) (112, 401), 2.146 (24) (330). The mineral is named in honor of the German amateur mineralogist Volker Betz (b. 1947).

Keywords: new mineral, betzite, quadridavyne, cancrinite group, crystal structure, IR spectroscopy, calcic xenolith, pyrometamorphism, Bellerberg paleovolcano, Eifel.

Introduction

Cancrinite-group minerals are microporous hexagonal or trigonal feldspathoids with negatively charged frameworks that consist of layers composed of six-membered rings of Si- and Al-centered tetrahedra perpendicular to the **c** axis and host alkali and alkaline-earth cations (mainly Na^+, K^+, Ca^{2+}), anions (Cl^-, SO_4^{2-}, CO_3^{2-}, SO_3^{2-}, PO_4^{3-}, $C_2O_4^{2-}$, OH^-, F^-, S_n^{m-}), and neutral molecules (H_2O and CO_2) in channels positioned along the [0 0 *z*] axis (Merlino 1984, Ballirano *et al*. 1996, Bonaccorsi & Merlino 2005, Pekov *et al*. 2011, Chukanov *et al*. 2021). Three different kinds of layers can be formed by six-membered rings of tetrahedra; these traditionally being denoted by the letters *A*, *B*, and *C* (Rinaldi & Wenk 1979, Ballirano *et al*. 1996). The simplest two-layer cancrinite (CAN)-type framework is characterized by an *AB* stacking sequence. Minerals with the CAN-type framework are the only representatives of the cancrinite group that contain channels 5.8 to 6.0 Å in diameter created by 12-membered rings (Fig. 1).

Twelve cancrinite-group minerals having aluminosilicate frameworks with the *AB* stacking sequence, including the new mineral species betzite described in this paper, are known. Nine of them have a shortened *a* parameter (a_{can} = 12.4–13.1 Å), while three others, namely pitiglianoite, microsommite, and quadridavyne, are characterized with their *a* values being multiples of this ($a = 2a_{can}$ for quadridavyne and $a = a_{can}\cdot 3^{1/2}$ for microsommite and pitiglianoite). Changes in *a* are a function of different ways in which nonequivalent channels alternate, this being a result of ordering of extra-framework components (Bonaccorsi & Merlino 2005). Betzite, ideally $Na_6Ca_2(Al_6Si_6O_{24})Cl_4$, is a dimorph of quadridavyne with a small cancrinite-type unit cell and equivalent wide channels.

Betzite is named in honor of the German amateur mineralogist Volker Betz (*b*. 1947). Mr. Betz is a well-known mineral collector, an author of numerous mineralogical publications, and a specialist in mineral photography. The new mineral and its name were approved by the IMA Commission on New Minerals, Nomenclature and Classification (IMA No. 2021-037). The type material is deposited in the Fersman Mineralogical Museum of the Russian Academy of Sciences, Moscow, Russia, under catalogue number 97677.

Occurrence, General Appearance, and Physical Properties

Betzite was discovered in calcic xenoliths contained within alkaline basalt of the Bellerberg paleovolcano, which is situated between Mayen and Kottenheim in the Laach Lake (Laacher See) area, Eastern Eifel region, Rhineland-Palatinate (Rheinland-Pfalz), Germany. The associated minerals are anorthite, phlogopite, diopside, grossular, fluorite, calcite, an insufficiently studied calcium hydrosilicate related to tobermorite, and accessory vanadoallanite-(Ce).

Betzite is considered to be a product of contact metamorphism (metasomatism) related to incorporation of a calcic xenolith in an alkaline basalt. It occurs as colorless hexagonal prismatic crystals up to 2 mm long and up to 0.5 mm thick (Fig. 2). Hexagonal prisms $\{10\bar{1}0\}$ and $\{11\bar{2}0\}$ are the major crystal forms, and numerous unspecified subordinate forms, mainly $\{h0\bar{l}m\}$, are observed on terminations. Microtwinning by merohedry Class I (Nespolo & Ferraris 2000) with an inversion center as a twinning operator was revealed during crystal-structure refinement.

Betzite is brittle, with a Mohs' hardness of 5½. Distinct cleavage on $\{10\bar{1}0\}$ and distinct parting on $\{0001\}$ are observed under the microscope on

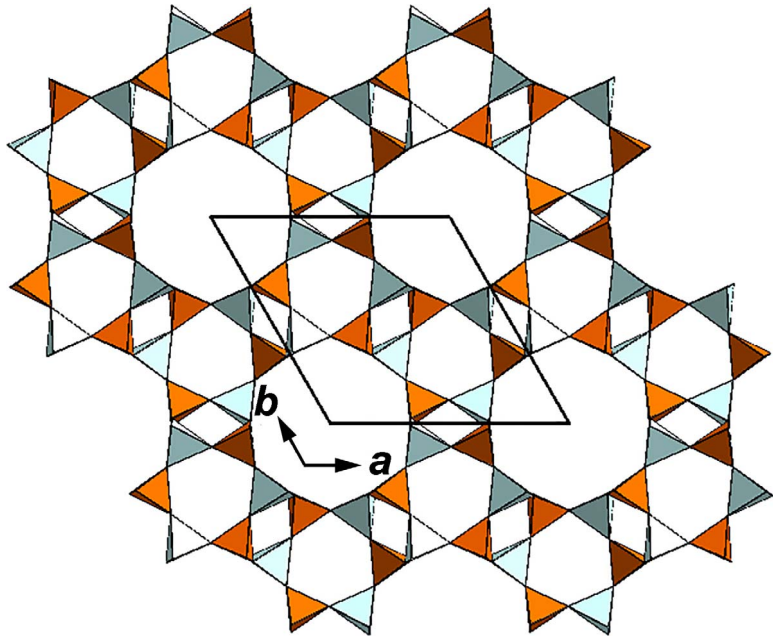

FIG. 1. The two-layer CAN-type framework composed of alternating SiO_4 (turquoise) and AlO_4 (orange) tetrahedra. The unit cell is outlined.

fragments with crystal forms. The density measured by flotation in heavy liquids (mixtures of bromoform and heptane) is 2.38(2) g/cm^3. The density calculated using the empirical formula and unit-cell volume refined from powder XRD data is 2.363 g/cm^3. The unit-cell volume determined from single-crystal XRD data was not used because single-crystal XRD data were obtained at a low temperature of 100 K.

Fluorescence was studied using an UV lamp VERSALUME (RAYTECH). Betzite is non-fluorescent under short-wave (with $\lambda = 245$ nm) and long-wave (with $\lambda = 330$ nm) UV radiation.

Optical properties were investigated using a suspension prepared from a powdered betzite sample and immersion liquids. The new mineral is optically uniaxial (+) with $\omega = 1.528(2)$ and $\varepsilon = 1.545(3)$ ($\lambda = 589$ nm). Under the microscope and plane polarized light betzite is nonpleochroic and colorless.

INFRARED SPECTROSCOPY

The IR absorption spectrum of betzite was obtained using mineral powder that was mixed with anhydrous KBr, pelletized, and then analyzed using an ALPHA FTIR spectrometer (Bruker Optics) which has a resolution of 4 cm^{-1}. A total of 16 scans were collected over the range 360–3800 cm^{-1}. The IR spectrum of an analogous (in weight and shape) pellet of pure KBr was used as a reference.

The IR spectra of betzite and the related mineral davyne, $(Na,K)_6Ca_2(Al_6Si_6O_{24})Cl_2(SO_4)$ (used for comparison), are given in Figure 3. The assignment of absorption bands in the IR spectrum of betzite is as follows (relative maximum absorbance units are given in parentheses):

- 3423 cm^{-1} – O–H stretching vibrations of H_2O molecules occurring in the channel (6%).
- 1621 cm^{-1} – bending vibrations of H_2O molecules (4%).
- 1111 cm^{-1} – asymmetric stretching mode of SO_4^{2-} [the degenerate $F_2(\nu_3)$ mode] overlapping with a band of stretching vibrations of the framework (50%).
- 1009 cm^{-1} – stretching vibrations of the aluminosilicate framework, possibly overlapping with a weak band of symmetric stretching band of SO_4^{2-} [the nondegenerate $A_1(\nu_1)$ mode] (100%).
- 550–670 cm^{-1} – mixed vibrations of the aluminosilicate framework. The weak band of bending vibrations of SO_4^{2-} [the degenerate $F_2(\nu_4)$ mode] could not be observed owing to overlap with the band at 612 cm^{-1} (11–22%).
- Below 470, 438, and 426 cm^{-1} – lattice modes involving bending vibrations of the aluminosilicate

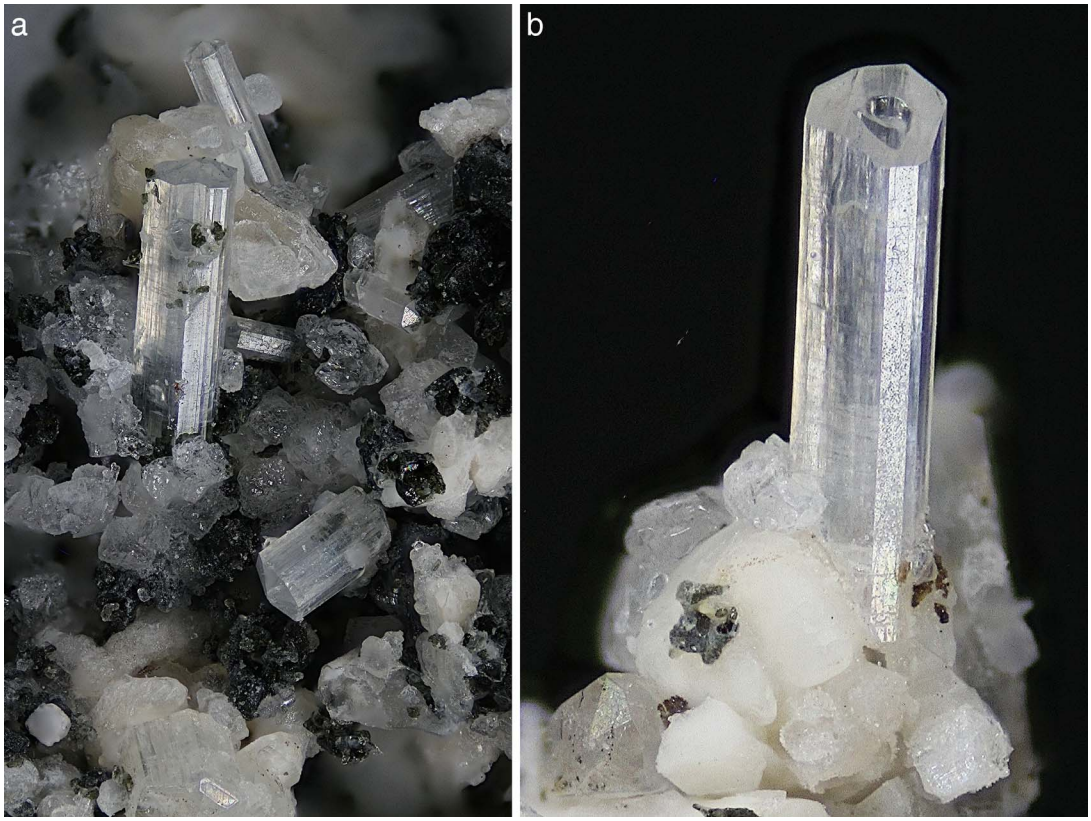

FIG. 2. Betzite crystals (colorless, prismatic) in association with anorthite (white) and diopside (dark green to black). FOV widths: (a) 1.4 mm and (b) 0.9 mm.

framework and libration vibrations of SO_4^{2-} and H_2O (28, 67, and 64%, respectively).

The band assignments were made following those provided in previous contributions related to cancrinite-group minerals (Chukanov *et al*. 2011a, 2021)

In the IR spectrum of davyne, as compared to betzite, the peak at 1111 cm^{-1} is better resolved and an additional band arising from $(SO_4)^{2-}$ is observed at 1161 cm^{-1}. The intensities of weak bands in the range 710–740 cm^{-1} in the IR spectra of minerals belonging to the betzite–davyne solid-solution series show a positive correlation with the content of sulfate groups (*i.e*., the intensities increase as does sulfate content). These bands are tentatively assigned to modes involving SO_4^{2-} libration (below 300 cm^{-1}) and bending vibrations of the aluminosilicate framework (at 425 and 438 cm^{-1}).

The absolute values of the absorption coefficients could not be calculated owing to the small amount of material used in obtaining the IR spectrum (~1 mg). However, in the IR spectrum of betzite, the ratio of the integrated peak intensity in the range 3000–3800 cm^{-1} compared to that of the band in the range 610–612 cm^{-1} (which was used as an internal standard) is about nine times greater than for davyne. This fact confirms the presence of significant amounts of H_2O in betzite measured by a direct method (see below).

Absorption bands corresponding to $(CO_3)^{2-}$ and CO_2 molecules are absent in the IR spectrum of betzite, suggesting neither is present.

CHEMICAL DATA

The chemical composition of betzite was determined using a Tescan VEGA-II XMU scanning electron microscope equipped with the energy dispersive spectrometer INCA Energy 450 (20 kV, 65–110 pA, 120 nm beam diameter).

The migration of alkalis under the electron beam during electron probe microanalyses (EPMA) of glasses and aluminosilicates has been well documented (Usher 1981, Natarajan 2000, Morgan & London 2005, Campbell *et al*. 2016). To investigate the

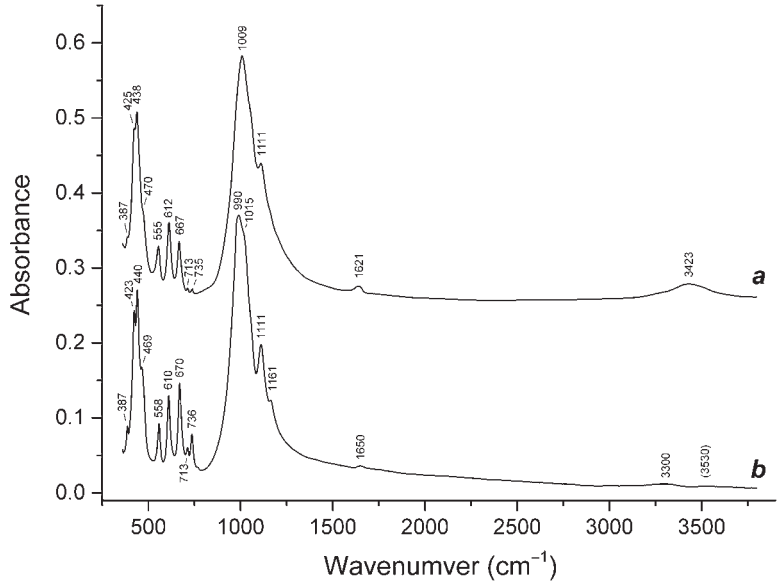

FIG. 3. Powder infrared absorption spectra of (a) betzite and (b) davyne (a sample close to endmember davyne with the empirical formula $Na_{5.4}Ca_{2.0}K_{0.8}(Si_{6.1}Al_{5.9}O_{24})Cl_{2.0}(SO_4)_{1.1}(OH,H_2O)_{\sim 0.1}$ and crystal chemical formula $[Ca_2Cl_2][Na_{5.2}K_{0.8}(SO_4)_{1.0}][Si_6Al_6O_{24}]$: Rozenberg *et al*. 2009) from the Sar-e Sang gem lazurite deposit, Afghanistan.

possibility of Na migration during EPMA analysis, measurements were made with a defocused beam over areas of both 5×5 μm^2 and 20×20 μm^2. These produced similar data (11.71 and 11.88 wt.%, respectively), suggesting no significant Na migration had occurred.

The H_2O content was determined by means of the modified Penfield method. CO_2 was not measured because, according to IR spectroscopic and structural data, carbonate groups and CO_2 molecules are not present in detectable amounts in betzite.

Five spot analyses were carried out on one grain, a portion of which was used for the single-crystal structure investigation. Analytical data are given in Table 2. No other elements with $Z > 8$ were found above detection limits.

The empirical formula, based on 12 framework cations (*i.e*., 12 T = Si+Al+Fe *apfu*, $Z = 1$), is $Na_{4.22}K_{1.13}Ca_{2.11}Mg_{0.06}(Si_{6.01}Al_{5.90}Fe^{3+}_{0.09}O_{24})Cl_{3.25}(SO_4)_{0.26}(H_{1.34}O_{0.64})$. This approach, rather than using one based on a fixed number of anions, facilitates evaluation of potential vacancies at the T sites. Taking into account structure data, the simplified formula can be written as $(Na,K,\square)_6Ca_2(Al_6Si_6O_{24})(Cl,SO_4,H_2O)_4$. The idealized formula is $Na_6Ca_2(Al_6Si_6O_{24})Cl_4$.

The Gladstone-Dale compatibility index, $1 - (K_p/K_c)$ (Mandarino 1981), is –0.035 (rated as excellent) using the density calculated using the crystal-chemical formula and unit-cell parameters refined from the powder X-ray diffraction data or –0.016 (rated as superior) using measured density.

X-RAY DIFFRACTION DATA AND CRYSTAL STRUCTURE

Powder X-ray diffraction (XRD) data were collected using a Rigaku R-AXIS Rapid II diffractometer (image plate), Co$K\alpha$, 40 kV, 15 mA, rotating anode with the microfocus optics, Debye-Scherrer geometry, d = 127.4 mm, exposure 15 min. The raw powder XRD data were collected using the program suite designed by Britvin *et al*. (2017). Calculated intensities were obtained by means of STOE WinXPOW *v*. 2.08 program suite based on the atomic coordinates and unit-cell parameters from the refined crystal structure[1].

Powder XRD data for betzite are given in Table 3. The indexed powder diffraction pattern gave the refined unit-cell parameters a = 12.876(2) Å, c = 5.361(2) Å, V = 769.7(4) Å^3.

Preliminary single-crystal X-ray diffraction studies were carried out at room temperature with an Xcalibur

[1] Supplementary Data are available from the Depository of Unpublished Data on the MAC website (http://mineralogicalassociation.ca/), document "Betzite, CM61, 22-00039".

TABLE 1. STRUCTURAL DATA, DATA COLLECTION INFORMATION, AND STRUCTURE REFINEMENT DETAILS FOR BETZITE

Formula	$Na_{4.20}K_{1.14}Ca_{2.12}(Si_6Al_6O_{24})Cl_{3.26}(SO_4)_{0.21}\cdot 0.54N_2O$
Formula weight	1084.90
Temperature, K	100(2)
Radiation and wavelength, Å	Mo$K\alpha$; 0.71073
Crystal system, space group, Z	Hexagonal, $P6_3$, 1
Unit-cell dimensions, Å	$a = 12.8166(9)$
	$c = 5.3562(3)$
V, Å^3	761.95(12)
Absorption coefficient μ, mm^{-1}	1.417
F_{000}	534
Crystal size, mm^3	$0.15 \times 0.19 \times 0.22$
Diffractometer	Xcalibur Eos CCD
Absorption correction	Multi-scan
θ range for data collection, °	4.225–28.281
Index ranges	$-13 \le h \le 17$, $-14 \le k \le 14$, $-4 \le l \le 7$
Reflections collected	2419
Independent reflections	1132 ($R_{int} = 0.0296$)
Independent reflections with $I > 2\sigma(I)$	1007
Refinement method	Full-matrix least-squares on F^2
Number of refined parameters	110
Final R indices [$I > 2\sigma(I)$]	$R_1 = 0.0407$, w$R_2 = 0.0703$
R indices (all data)	$R_1 = 0.0464$, w$R_2 = 0.0732$
GoF	1.075
Largest diff. peak and hole, e/Å^3	0.47 and −0.65

Oxford Diffraction diffractometer equipped with a CCD detector using the ω scanning mode. These data are published elsewhere (Chukanov *et al*. 2011b). Final single-crystal X-ray diffraction studies were carried out at 100 K, details of which are provided in Table 1. The crystal structure of betzite was solved by direct methods and refined using programs in the SHELX package (Sheldrick 2008, 2015).

The crystal structure of betzite (Fig. 4, Tables 4 and 5) is based on the CAN-type framework (Fig. 1) constructed of SiO_4 and AlO_4 tetrahedra arranged in a simple *AB* stacking sequence of six-membered rings of tetrahedra along the **c** axis. The Si and Al atoms are ordered over the two tetrahedral sites within the framework, based on average cation–anion distances in the tetrahedra (Si–O = 1.620 Å, Al–O = 1.729 Å).

TABLE 2. CHEMICAL COMPOSITION OF BETZITE

Constituent	wt.%	Range	SD	Probe Standard
Na_2O	11.88	11.16–12.27	0.40	Albite
K_2O	4.82	4.30–6.10	0.71	Sanidine
CaO	10.74	10.39–11.05	0.22	Wollastonite
MgO	0.21	0.11–0.31	0.08	MgO syn.
Al_2O_3	27.32	26.29–27.96	0.48	Al_2O_3 syn.
Fe_2O_3	0.68	0.42–0.82	0.15	Fe
SiO_2	32.84	32.31–33.62	0.29	SiO_2
SO_3	1.89	1.63–2.22	0.22	FeS_2
Cl	10.48	10.15–10.80	0.24	NaCl
H_2O	1.10			
$-O\equiv Cl$	−2.37			
Total	99.59			

TABLE 3. POWDER X-RAY DIFFRACTION DATA (d IN Å) FOR BETZITE

I_{obs}	d_{obs}	I_{calc}*	d_{calc}**	h k l	I_{obs}	d_{obs}	I_{calc}*	d_{calc}**	h k l
31	**11.14**	63	11.100	100	13	1.933	19	1.927	402
14	6.43	16	6.408	110	4	1.876	5	1.868	511
93	**4.833**	90	4.824	101	2	1.856	2	1.850	600
7	4.213	3	4.195	210	3	1.833	3	1.825	340
2	4.126	1	4.110	111	18	1.802	26	1.796	142
95	**3.715**	89	3.670	300	3	1.786	3	1.777	250
100	**3.313**	100	3.303	211	3	1.766	4	1.763	103
3	3.218	2	3.204	220	8	1.735	11	1.727	431
13	3.092	12	3.078	310	1	1.695	1	1.700	203
5	3.054	4	3.044	301	1	1.675	3	1.670	332
37	**2.787**	38	2.775	400	6	1.646	2	1.651	242
56	**2.681**	47	2.678	002			9	1.643	123
		25	2.669	131	8	1.610	4	1.614	611
8	2.607	10	2.603	102			12	1.602	440
35	**2.474**	4	2.471	112	2	1.593	2	1.586	700
		37	2.464	401	2	1.548	4	1.544	133
3	2.433	6	2.422	140	6	1.527	3	1.522	602
2	2.308	4	2.300	321			7	1.520	531
1	2.216	1	2.220	500	5	1.505	2	1.508	342
		1	2.207	411			10	1.501	403
4	2.175	6	2.169	302	2	1.477	1	1.479	621
24	2.146	30	2.136	330			5	1.470	170
3	2.107	2	2.098	420	1	1.394	3	1.387	800
11	2.061	12	2.055	222	11	1.380	22	1.375	442
5	2.026	5	2.021	132	8	1.349	16	1.343	801
2	1.962	2	1.953	421					

The strongest diagnostic reflections are highlighted in bold type.

* For the calculated pattern, only reflections with intensities $\geq$1 are given.

** For the unit-cell parameters calculated from single-crystal data.

TABLE 4. FRACTIONAL COORDINATES, DISPLACEMENT PARAMETERS OF ATOMS (U IN Å^2), AND SITE OCCUPANCY FACTORS (s.o.f.) IN THE STRUCTURE OF BETZITE

Site	x	y	z	U_{eq}/U_{iso}*	s.o.f.
Al	0.07347(12)	0.41174(12)	0.7606(3)	0.0065(3)	$Al_{1.00}$
Si	0.33174(11)	0.41287(12)	0.7602(3)	0.0077(3)	$Si_{1.00}$
O1	0.2110(3)	0.4211(3)	0.7152(6)	0.0138(8)	$O_{1.00}$
O2	0.1136(3)	0.5617(3)	0.7487(8)	0.0149(7)	$O_{1.00}$
O3	0.0109(4)	0.3408(4)	0.0416(5)	0.0149(9)	$O_{1.00}$
O4	0.3244(4)	0.3486(4)	0.0250(5)	0.0143(9)	$O_{1.00}$
CAN cage					
Ca	2/3	1/3	0.2167(3)	0.0096(4)	$Ca_{1.00}$
Cl	0.322(6)	0.6366(17)	0.2210(7)	0.028(3)	$Cl_{0.33}$
Wide channel					
Na1	0.1425(11)	0.2942(10)	0.288(3)	0.022(3)	$Na_{0.31}Ca_{0.02}$
Na2	0.1737(12)	0.3477(11)	0.282(3)	0.023(3)	$Na_{0.34}$
K	0.1091(7)	0.2248(8)	0.2880(17)	0.0301(17)	$K_{0.19}Na_{0.05}(H_2O)_{0.09}$
S	0.0	0.0	0.302(9)	0.077(12)*	$S_{0.105}$
OS	0.0	0.0	0.563(9)	0.077(12)*	$O_{0.105}$
OS1	0.893(5)	0.889(4)	0.234(19)	0.10(2)*	$O_{0.105}$
Cl1	0.078(3)	0.130(3)	0.312(6)	0.102(9)*	$Cl_{0.13}$
Cl2	0.916(6)	1.038(7)	0.005(11)	0.14(2)*	$Cl_{0.08}$

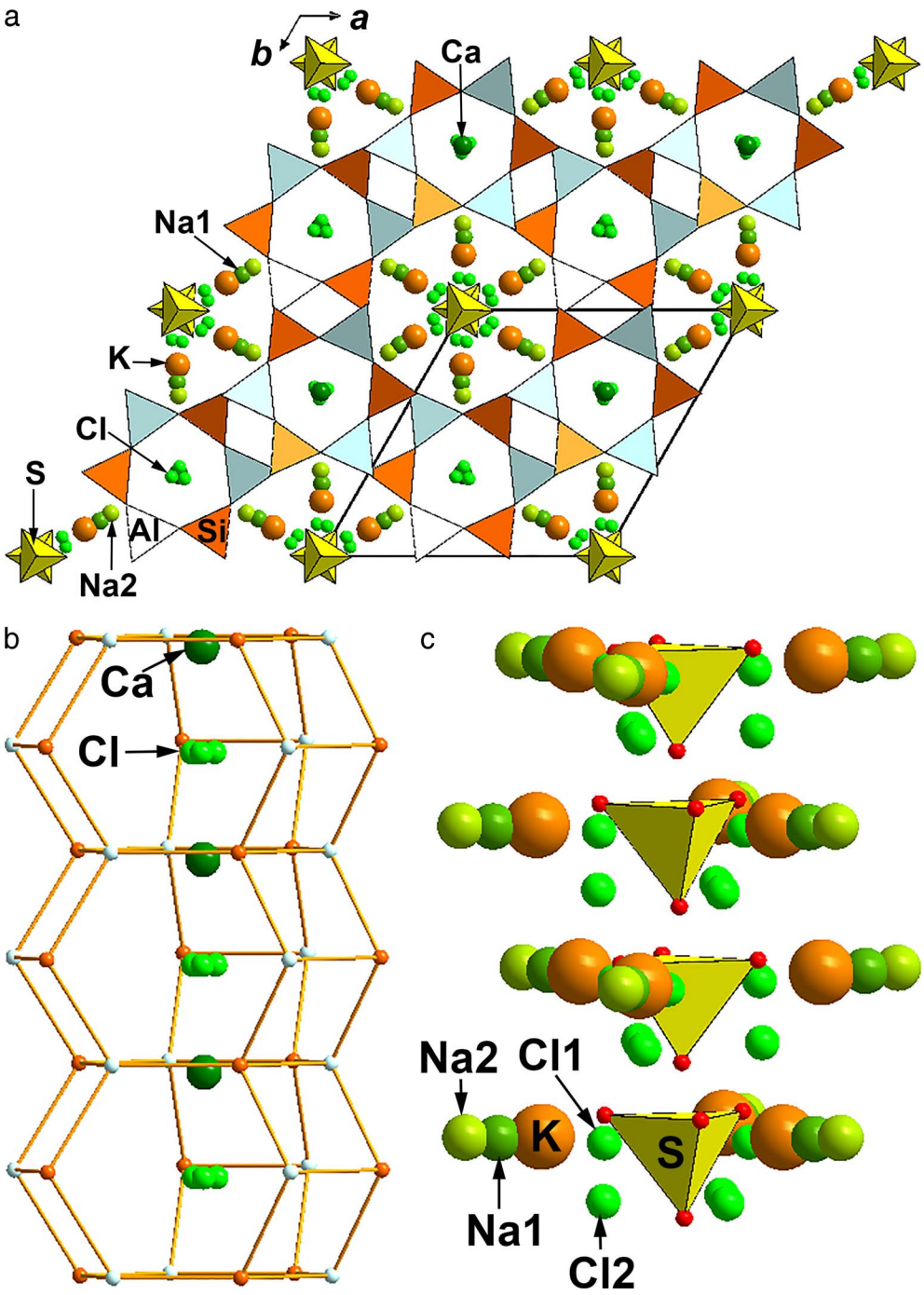

FIG. 4. The crystal structure of betzite: (a) general view (the unit cell is outlined), (b) the column of cancrinite cages hosting alternating Ca^{2+} and Cl^{-} ions (the Al and Si atoms are shown with small orange and blue balls), and (c) the arrangement of the extra-framework components in the wide channel.

TABLE 5. SELECTED INTERATOMIC DISTANCES (Å) IN BETZITE

Ca	– O2	2.446(4) × 3	Na2	– O4	2.367(17)
	– Cl	2.676(4)		– O3	2.415(18)
	– Cl	2.722(4)		– Cl1	2.43(3)
	– O1	2.725(3) × 3		– O1	2.460(18)
				– O3	2.657(18)
Al	– O1	1.723(4)		– O4	2.731(17)
	– O2	1.724(4)		– OS1	2.78(7)
	– O3	1.734(4)		– Cl2	2.79(7)
	– O4	1.735(4)		– O1	3.142(19)
Si	– O2	1.616(4)	K	– Cl2	2.42(8)
	– O4	1.619(3)		– O3	2.721(9)
	– O1	1.621(4)		– OS	2.77(2)
	– O3	1.625(4)		– O4	2.782(9)
				– OS1	2.79(9)
S	– OS	1.401(14)		– OS1	2.86(8)
	– OS1	1.447(14) × 3		– Cl2	2.87(7)
				– O4	2.887(9)
Na1	– OS1	2.20(7)		– OS	2.90(3)
	– O3	2.440(16)		– O3	2.912(10)
	– O4	2.506(15)		– O1	3.160(10)
	– O4	2.674(15)		– Cl1	3.22(3)
	– O1	2.688(16)		– OS1	3.30(10)
	– O3	2.710(15)		– Cl1	3.33(4)
	– Cl2	2.98(8)			
	– OS1	3.22(8)			

Note: All possible Na–(O/Cl) and K–(O/Cl) contacts are listed.

Narrow channels (columns of cancrinite cages) host alternating Ca and Cl^- ions, giving rise to alternating ...Ca···Cl···Ca···Cl... chains along [001], with Ca at the bases of the cancrinite cages and Cl (disordered at a split site) at the centers of cancrinite cages, which are located along the three-fold axis (Fig. 4b). These channels host SO_4^{2-} groups, Cl^- anions, and three split sites statistically occupied by Na, K, and Ca (these statistically divided over three split sites) and water molecules (Table 4 and Fig. 4c).

Discussion

The unit-cell parameters of most minerals with $P6_3$ symmetry and the CAN-type framework, vary in the ranges of $a = 12.4$–13.1 Å, $c = 5.0$–5.4 Å. However, specific features, related to the ordering of extra-framework components, may result in superstructures with unit cells based on multiples of a, and thus expanded unit-cell volumes. In particular, the unit-cell parameters of microsommite (Bonaccorsi *et al*. 2001) and pitiglianoite (Merlino *et al*. 1991), which possess superstructures based on the cancrinite crystal structure with simple *AB*-type stacking, are $a_{mic} = a_{can} \cdot 2\sin(60°)$, $c_{mic} = c_{can}$, whereas in quadridavyne (Bonaccorsi *et al*. 1994) they are $a_{qua} = 2a_{can}$, $c_{mic} = c_{can}$.

The dimorphous pairs, davyne and microsommite, $(Na,K)_6Ca_2(Si_6Al_6O_{24})Cl_2(SO_4)$, as well as vishnevite and pitiglianoite, $[(Na,K)_8(Si_6Al_6O_{24})(SO_4)\cdot 2H_2O$, are each differentiated on the basis of their respective ordering schemes of the extra-framework components they contain. Within this context, betzite and quadridavyne, both ideally $Na_6Ca_2(Al_6Si_6O_{24})Cl_4$, constitute another dimorphous pair having the CAN-type framework. The two minerals differ based on the nature of the channels they contain: in betzite there is only one unique channel (Fig. 4a), while in quadridavyne, there are two such channels, these being arranged in a regular, alternating manner (Fig. 5). Comparative data for betzite and other Cl-bearing cancrinite-group minerals having the CAN-type framework (with the *AB* stacking sequence) are given in Table 6. Among these minerals, betzite is characterized by the largest ε refractive index and the highest birefringence.

Acknowledgments

The authors are grateful to two anonymous reviewers and Associate Editor Henrik Friis for

TABLE 6. COMPARATIVE DATA FOR Cl-BEARING CANCRINITE-GROUP MINERALS WITH CAN-TYPE FRAMEWORK

Mineral	Betzite	Quadridavyne	Davyne	Balliranoite	Microsommite
Simplified formula	$Na_6Ca_2(Al_6Si_6O_{24})Cl_4$	$Na_6Ca_2(Al_6Si_6O_{24})Cl_4$	$Na_6Ca_2(Si_6Al_6O_{24})Cl_2(SO_4)$	$Na_6Ca_2(Si_6Al_6O_{24})Cl_2(CO_3)$	$Na_6Ca_2(Si_6Al_6O_{24})Cl_2(SO_4)$
Space group	$P6_3$	$P6_3/m$	$P6_3$	$P6_3$	$P6_322$
a, Å	12.8166	25.771	12.67–12.85	12.695	22.08
c, Å	5.3562	5.371	5.32–5.37	5.325	5.33
V, Å^3	761.95	3089	740–768	743.2	2250
Z	1	4	1	1	3
Strong lines of the powder X-ray diffraction pattern: *d*, Å (*I*, %)					
	11.14 (31)	4.80 (s)	4.80 (100)	4.797 (100)	4.81 (100)
	4.833 (93)	3.71 (vs)	3.671 (100)	3.669 (57)	3.69 (100)
	3.715 (95)	3.31 (vs)	3.283 (100)	3.281 (73)	3.29 (100)
	3.313 (100)	2.788 (s)	2.756 (50)	2.754 (16)	2.765 (60)
	2.787 (37)	2.677 (m)	2.670 (60)	2.662 (58)	2.670 (80)
	2.681 (56)	2.474 (m)	2.447 (50)	2.446 (31)	2.660 (80)
	2.474 (35)	2.147 (m)	2.121 (60)	2.120 (18)	2.455 (60)
	2.146 (24)				
Optical data	Uniaxial (+)	Uniaxial (+)	Uniaxial (+)	Uniaxial (+)	Uniaxial (+)
	$\omega = 1.528$	$\omega = 1.529$	$\omega = 1.518–1.519$	$\omega = 1.523$	$\omega = 1.521$
	$\varepsilon = 1.545$	$\varepsilon = 1.532$	$\varepsilon = 1.519–1.528$	$\varepsilon = 1.525$	$\varepsilon = 1.529$
Density, g/cm^3	2.38 (meas.)	2.335 (meas.)	2.43–2.53 (meas.)	2.48 (meas.)	2.42–2.53 (meas.)
	2.363 (calc.)	2.354 (calc.)	2.50 (calc.)	2.486 (calc.)	2.48 (calc.)
Sources	This work	Bonaccorsi *et al.* 1994; Ballirano *et al.* 1996; Bokiy & Borutskiy 2003	Bonaccorsi *et al.* 1990, 1991; Hassan & Grundy 1990; Ballirano *et al.* 1996; Bokiy & Borutskiy 2003; Rozenberg *et al.* 2009	Chukanov *et al.* 2010	Bonaccorsi *et al.* 2001; Bokiy & Borutskiy 2003

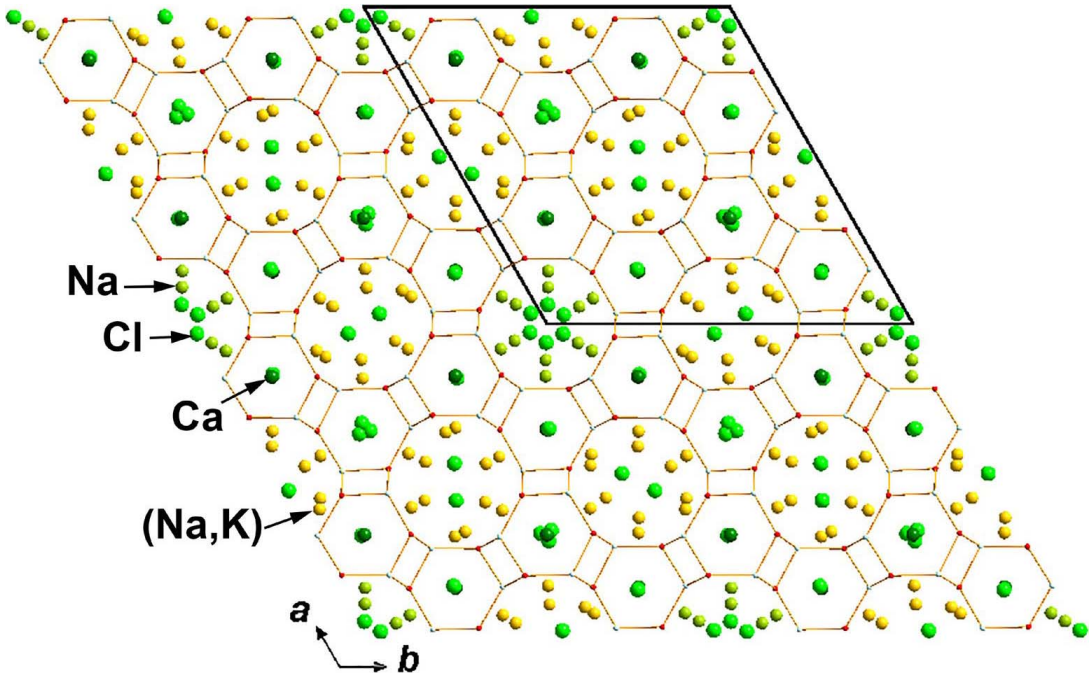

FIG. 5. Alternation of two types of wide channels in the structure of quadridavyne (drawn using data from Bonaccorsi *et al.* 1994). The unit cell is outlined.

valuable comments. Powder and single-crystal X-ray diffraction studies, crystal structure refinement, determination of water, and IR spectroscopic investigation were supported by the Russian Science Foundation, grant No. 22-17-00006. Collecting of minerals, their identification, and electron microprobe analyses were carried out in accordance with the state task, state registration No. AAA-A19-119092390076-7. Technical support by the SPbSU X-Ray Diffraction Research Resource Center in the powder X-ray diffraction studies is acknowledged.

REFERENCES

BALLIRANO, P., MARAS, A., & BUSECK, P.R. (1996) Crystal chemistry and IR spectroscopy of Cl- and SO_4-bearing cancrinite-like minerals. *American Mineralogist* **81**, 1003–1012. DOI: https://doi.org/10.2138/am-1996-7-822

BOKIY, G.B. & BORUTSKIY, B.E. (2003) *Minerals Vol.2: Framework Silicates*. Nauka, Moscow, Russia (in Russian).

BONACCORSI, E., MERLINO, S., & PASERO, M. (1990) Davyne: Its structural relationships with cancrinite and vishnevite. *Neues Jahrbuch fur Mineralogie, Monatshefte* **1990**, 97–112.

BONACCORSI, E., MERLINO, S., & PASERO, M. (1991) Davyne from Zabargad (St. John's) Island: Peculiar chemical and structural features. *Acta Vulcanologica* **2**, 55–63.

BONACCORSI, E., MERLINO, S., ORLANDI, P., PASERO, M., & VEZZALINI, G. (1994) Quadridavyne, $[(Na,K)_6Cl_2][Ca_2Cl_2][Si_6Al_6O_{24}]$, a new feldspathoid mineral from Vesuvius area. *European Journal of Mineralogy* **6**, 481–488. DOI: https://doi.org/10.1127/ejm/6/4/0481

BONACCORSI, E., MERLINO, S., PASERO, M., & MACEDONIO, G. (2001) Microsommite: Crystal chemistry, phase transitions, Ising model and Monte Carlo simulations. *Physics and Chemistry of Minerals* **28**, 509–522. DOI: https://doi.org/10.1007/s002690100179

BONACCORSI, E. & MERLINO S. (2005) Modular microporous minerals: Cancrinite-davyne group and C-S-H phases, *Reviews in Mineralogy and Geochemistry* **57**, 241–290. DOI: https://doi.org/10.2138/rmg.2005.57.8

BRITVIN, S.N., DOLIVO-DOBROVOLSKY, D.V., & KRZHIZHANOVSKAYA, M.G. (2017) Software for processing the X-ray powder diffraction data obtained from the curved image plate detector of Rigaku RAXIS Rapid II diffractometer. *Zapiski Rossiiskogo Mineralogicheskogo Obshchestva* **146**(3), 104–107 (in Russian).

CAMPBELL, L.S., CHARNOCK, J., DYER, A., HILLIER, S., CHENERY, S., STOPPA, F., HENDERSON, C.M.B., WALCOTT, R., &

Rumsey, M. (2016) Determination of zeolite-group mineral compositions by electron probe microanalysis. *Mineralogical Magazine* **80**, 781–807. DOI: https://doi.org/10.1180/minmag.2016.080.044

Chukanov, N.V., Zubkova, N.V., Pekov, I.V., Olysych, L.V., Bonaccorsi, E., & Pushcharovsky, D.Yu. (2010) Ballirianoite, $(Na,K)_6Ca_2(Si_6Al_6O_{24})Cl_2(CO_3)$, a new cancrinite-group mineral from Monte Somma Vesuvio volcanic complex, Italy. *European Journal of Mineralogy* **22**, 113–119. DOI: https://doi.org/10.1127/0935-1221/2010/0022-1983

Chukanov, N.V., Pekov, I.V., Olysych, L.V., Zubkova, N.V., & Vigasina, M.F. (2011a) Crystal chemistry of cancrinite-group minerals with AB-type frameworks. II. IR spectroscopy and its crystal chemical implications: review and new data. *The Canadian Mineralogist* **49**, 1151–1164. DOI: https://doi.org/10.3749/canmin.49.5.1151

Chukanov, N.V., Pekov, I.V., Zubkova, N.V., & Pushcharovsky, D.Yu. (2011b) Crystal chemistry of a new variety of quadridavyne. *In* Abstracts of VI International Symposium "Mineral Diversity, Research and Preservation". Sofia, October 7th–10th, 2011. Sofia: Earth and Man Foundation.

Chukanov, N.V., Aksenov, S.M., & Rastsvetaeva, R.K. (2021) Structural chemistry, IR spectroscopy, properties, and genesis of natural and synthetic microporous cancrinite- and sodalite-related materials: A review. *Microporous and Mesoporous Materials* **323**, 111098. DOI: https://doi.org/10.1016/j.micromeso.2021.111098

Hassan, I. & Grundy, H.D. (1990) Structure of davyne and implications for stacking faults. *The Canadian Mineralogist* **28**, 341–349.

Mandarino, J.A. (1981) The Gladstone-Dale relationship. IV. The compatibility concept and its application. *The Canadian Mineralogist* **41**, 989–1002.

Merlino, S. (1984) Feldspathoids: Their Average and Real Structures. *In* Feldspars & Feldspathoids (W.L. Brown, ed.). NATO ASI Series C: Mathematical and Physical Sciences vol 137. Springer, Dordrecht, Netherlands (435–470). DOI: https://doi.org/10.1007/978-94-015-6929-3_12

Merlino, S., Mellini, M., Bonaccorsi, E., Pasero, M., Leoni, L., & Orlandi, P. (1991) Pitiglianoite, a new feldspathoid from southern Tuscany, Italy: Chemical composition and crystal structure. *American Mineralogist* **76**, 2003–2008.

Morgan, G.B. & London, D. (2005) Effect of current density on the electron microprobe analysis of alkali aluminosilicate glasses. *American Mineralogist* **90**, 1131–1138. DOI: https://doi.org/10.2138/am.2005.1769

Natarajan, R. (2000) Migration of sodium in feldspar by electron beam – an experimental study. *Microscopy and Microanalysis* **6**(S2), 410–411. DOI: https://doi.org/10.1017/S1431927600034541

Nespolo, M. & Ferraris, G. (2000) Twinning by syngonic and metric merohedry. Analysis, classification and effects on the diffraction pattern. *Zeitschrift für Kristallographie - Crystalline Materials* **215**(2), 77–81. DOI: https://doi.org/10.1524/zkri.2000.215.2.77

Pekov, I.V., Olysych, L.V., Chukanov, N.V., Zubkova, N.V., Pushcharovsky, D.Yu., Van K.V., Giester G., & Tillmanns E. (2011) Crystal chemistry of cancrinite-group minerals with AB-type frameworks. I. Chemical and structural variations: Review and new data. *The Canadian Mineralogist* **49**, 1129–1150. DOI: https://doi.org/10.3749/canmin.49.5.1129

Rinaldi, R. & Wenk, H.R. (1979) Stacking variations in cancrinite minerals, *Acta Crystallographica, Section A* **35**, 825–828. DOI: https://doi.org/10.1107/S0567739479001868

Rozenberg, K.A., Rastsvetaeva, R.K., & Chukanov, N.V. (2009) Crystal structures of oxalate-bearing cancrinite with an unusual arrangement of CO_3 groups and sulfate-rich davyne. *Crystallography Reports* **54**(5), 793–799. DOI: https://doi.org/10.1134/S1063774509050101

Sheldrick, G.M. (2008) A short history of SHELX. *Acta Crystallographica* **A64**, 112–122. DOI: https://doi.org/10.1107/S0108767307043930

Sheldrick, G.M. (2015) Crystal structure refinement with SHELXL. *Acta Crystallographica* **C71**, 3–8. DOI: https://doi.org/10.1107/S2053229614024218

Usher, D.M. (1981) Sodium ion migration in glass on electron beam irradiation. *Journal of Physics C: Solid State Physics* **14**, 2039–2048.

Received June 14, 2022. Revised manuscript accepted September 16, 2022.

This manuscript was handled by Associate Editor Henrik Friis and Editor Andrew McDonald.